AD_____

Award Number: **W81XWH-07-2-0020**

TITLE: Molecular Evolution of Human PON to Design Enhanced Catalytic Efficiency for Hydrolysis of Nerve Agents

PRINCIPAL INVESTIGATOR: Dan Tawfik (Ph.D.) and J.L. Sussman (Ph.D.)

CONTRACTING ORGANIZATION: Weizmann Institute of Science, Rehovot 76100, Israel

REPORT DATE: February 2010

TYPE OF REPORT: Annual Report

PREPARED FOR: U.S. Army Medical Research and Materiel Command
Fort Detrick, Maryland 21702-5012

REPORT DOCUMENTATION PAGE

Form Approved
OMB No. 0704-0188

1. REPORT DATE *(DD-MM-YYYY)*	2. REPORT TYPE	3. DATES COVERED *(From - To)*
01-02-2010	Annual	31 JAN 2009 - 28 JAN 2010

4. TITLE AND SUBTITLE
Molecular Evolution of Human PON to Design Enhanced Catalytic Efficiency for Hydrolysis of Nerve Agents

5a. CONTRACT NUMBER

5b. GRANT NUMBER
W81XWH-07-2-0020

5c. PROGRAM ELEMENT NUMBER

6. AUTHOR(S)
Dr. Dan Tawfik (PhD)
Dr. Joel L. Sussman (PhD)

5d. PROJECT NUMBER

5e. TASK NUMBER

5f. WORK UNIT NUMBER

7. PERFORMING ORGANIZATION NAME(S) AND ADDRESS(ES)
Weizmann Institute of Science, Rehovot 76100 ISRAEL

8. PERFORMING ORGANIZATION REPORT NUMBER

9. SPONSORING / MONITORING AGENCY NAME(S) AND ADDRESS(ES)
US Army Medical Research and Material Command
Fort Detrick, Maryland 21702-5012

10. SPONSOR/MONITOR'S ACRONYM(S)

11. SPONSOR/MONITOR'S REPORT NUMBER(S)

12. DISTRIBUTION / AVAILABILITY STATEMENT
x approved for public release; distribution unlimited

13. SUPPLEMENTARY NOTES

14. ABSTRACT

Project Summary: The long-term objective of this effort is to develop a generic gene shuffling-based technology to rapidly screen libraries of 10^{10} proteins/peptides encoded by DNA libraries, for identifying biomolecules that can intercept both existing and emerging organophosphate-based chemical warfare nerve agents (CWNA). All 3rd year milestones have been met, and additional tasks were performed to advance the goals of the project:(a) Plasmids of mutants 8C8, 2H4, and 1G3 were delivered for further evaluation against authentic nerve agents at USAMRICD. In addition, on early March 2009, 9 mutants were expressed and purified in our laboratory and transferred to USAMRICD. (b) Two mutants which displayed enhanced hydrolysis properties were over expressed, crystallized, and their 3D structure revealed movements of the catalytic Ca^{2+} and amino acid side chains coordinating to the catalytic calcium. (c)*In vitro* and *in vivo* studies demonstrated improved thermostability and antidotal efficacy of wt rePON1 compared to human PON1. (d) Stereo-specific protocols were developed for the synthesis of enantiomers of coumarin surrogates of nerve agents (e) A Protocol was developed for a safe *in situ* procedure for fluoridation of coumarin analogs of nerve agents thus permitting direct selection of clones by use of G-agents and the interception technique. **Relevance**: This technology is envisaged to provide rapid discovery of pretreatment and post challenge therapeutic drugs against existing & emerging CWNA threats and will shorten the time from emergence of a threat to identification of potential counter-measures to a few days or weeks.

15. SUBJECT TERMS Directed evolution, X-ray crystallography, organophosphates & bioscavangers

16. SECURITY CLASSIFICATION OF:			17. LIMITATION OF ABSTRACT	18. NUMBER OF PAGES	19a. NAME OF RESPONSIBLE PERSON
					USAMRMC
a. REPORT U	b. ABSTRACT U	c. THIS PAGE U	UU	22	19b. TELEPHONE NUMBER *(include area code)*

Table of Contents

Introduction

Our objective is to generate by directed evolution combined with molecular design, the next generation of prophylactic antidotes against chemical warfare nerve agents. These will be catalytic bioscavengers possessing favorable bio-pharmaceutical properties and capable of hydrolyzing both G- and V-type nerve agents at such rates that will qualify them as drug candidates to be used as prophylactic and hopefully also as post treatment countermeasures against nerve agents intoxication. .

The full protection of animals against multiple LD_{50} doses of nerve agents by pretreatment with stoichiometric scavengers such as acetyl- and butyrylcholinestersaes (AChE / BChE,) requires, for example, enhancement of human blood levels of BChE by hundreds mg of exogenously administered human BChE. Thus, the development of catalytic bioscavengers that will permit reasonable protection against G- and V-type chemical warfare intoxication by pretreatment with a substantially lower dose regimen of protein became a mission of high priority. Mammalian paraoxonases (PON1)) became the choice for such endeavor. Yet, for PON1 wt enzymes to be considered as realistic antidotes, the catalytic proficiency requires substantial enhancement of k_{cat}/K_m when reacting with the toxic component of the racemic mixtures of G and V nerve agents.

Over the last 3 years we have demonstrated the potential of directed evolution, combining random and designed mutations based on 3D structures, to generate mutants of a recombinant mammalian PON1 (rePON1) with catalytic proficiency well above the wild type proficiency. We have evolved mutants that hydrolyze more than 10^5-fold faster the toxic isomers of the nerve agents surrogate coumarin-based compounds, when compared to rePON1 and human PON1. We also developed a safe in situ protocol for generating the corresponding fluoridates (i.e., the threat G agents), and showed that k_{cat}/K_m for these variants are as high as $1\text{-}2\text{x}10^7$ $M^{-1}min^{-1}$, a value that approaches the theoretical estimated minimal requirement for efficient prophylactic protection at reasonable doses (~50 mg/70 kg) without the need for post exposure therapy. The 3rd annual report describes the achievements of the 3rd year highlighted by identification of at least nine potential drug candidates that were over expressed in *E. coli*, purified and transferred to USAMRICD for testing with authentic nerve agents.

Body

I. Specific Aims

1. The development of high-throughput-assays for OP hydrolase variants exhibiting high specificity factors and turnover.

2. Provision of proof-of-concept for the proposed core technology employing directed evolution of new recombinant PON and AChE variants.

3. Isolation of interceptors for G- and V-type nerve agents, and expression in soluble form.

4. Design, generation and selection of 2nd generation libraries for V- and G-type agents.

5. Large-scale production of selected enzyme candidates, and their kinetic, structural and pharmacological evaluation

6. Establishment of "off-the-shelf" libraries for rapid identification of antidotes against emerging future threats

II. Significance to the goals of Counter ACT

The proposed approach opens new opportunities for rapid identification, characterization and implementation of novel countermeasures against CW agents. It will significantly decrease the time interval between the appearance of a new threat and discovery of potential antidotes to counteract it. The major benefits will be one or more products capable of efficient catalytic hydrolysis of G- and V-type nerve agents, as well as gene libraries derived from existing enzymes that can be used "off-the-shelf" to isolate new protein variants for almost any nerve agent or toxic industrial chemical serving as a target for the screen.

III. Year 03 Milestones

In general all 3rd year milestones were met, and well beyond.

03 Milestone #1: Develop at least two promising PON1 candidates capable of hydrolyzing the P(-) isomers of methylphosphonyl coumarin analogs of nerve agents

In the 3rd year, special emphasis was placed on reversal of the stereo-selectivity of rePON1, so as to yield variants capable of hydrolyzing the toxic isomers of nerve agents with high values of k_{cat}/K_m. Milestone #1 success criteria were:

a) PON1 mutants should display k_{cat}/K_m values $>10^5$ $M^{-1}min^{-1}$ towards (-)-OPs (viz., >2,000-fold greater than the wt enzyme), and we also proposed to:

b) Obtain at least one additional PON1 candidate with $k_{cat}/K_m > 2x10^7$ $M^{-1}min^{-1}$ when acting upon racemic methylphosphonyl coumarin analogs

Our screening for reversed stereo-selectivity of PON1 variants towards chiral OPs utilized the (-) optical isomer of $CH_3P(O)(OiPr)–X$ (IMP), and $CH_3P(O)(O\text{-cyclohexyl})–X$ (CMP), where the leaving group, X, is 3-cyano-7-hydroxy-4-methylcoumarin. (-)-IMP and (-)-CMP were obtained by treatment of the corresponding racemic OP ligands with the 3B3 rePON1 mutant, which hydrolyzes almost exclusively the (+)- isomers. In addition, (-)-CMP was isolated (on a 30-50 mg scale) by a chemo-enzymic procedure in which the non-hydrolyzed (-)-CMP residue from incubation of a 120 mg racemic mixture of CMP with the 3B3 mutant was extracted into chloroform, and then washed with a bicarbonate solution to remove excess of the free leaving group, 3-cyano-7-hydroxy-4-methylcoumarin. The (-)-CMP obtained after evaporation of the organic solvent was then crystallized; X-ray analysis confirmed the S_P absolute configuration of the toxic (-)-CMP isomer (Fig. 1). The relatively small background fluorescence due to the presence of <1.5 % of free coumarin, and the absence of the (+) isomer, permitted meaningful and efficient FACS sorting of clones of variants capable of reversing the stereo-preference of rePON1 (Fig. 2), as well as unambiguous determination of their K_m and k_{cat} values for the toxic isomer. The new FACS-screened protocol based on the crystallized (-)-CMP expedited selection of active variants from 10^6-size libraries.

The enhanced evolution pathways for isolation of clones capable not only of reversing the stereo-preference from the (+) to the (-) isomer, but also of displaying high catalytic proficiency towards the toxic isomer, employed several engineering methodologies. We started from designed mutations based on the wt G3C9 variant. Thus, the double-mutant, H115W/V346A, was used to construct a 1st generation library containing mutants with up to 7-fold improved activity relative to H115W/V346A. Screening with (-)-IMP revealed that the F222S mutation is present in most of the improved clones. In a second round of mutagenesis, selecting with (-)-IMP, V346A disappeared from active clones, while H115W and F222S were retained. The next round of mutagenesis, to produce a 3rd generation library, involved screening with both (-)-IMP and (-)-CMP, thus permitting selection of mutants with preferential action on one or the other of these two model compounds. Thus, 3A7 was ~9 fold more active on (-)-IMP compared to (-)-

CMP, while 8C8 displayed ~ 4-fold enhanced efficiency towards (-)-CMP relative to (-)-IMP. The latter mutant displayed a remarkable reversed stereo-selectivity towards the toxic (-)-CMP, with a k_{cat}/K_m of ~ 10^5 $M^{-1}min^{-1}$ (Fig. 3 & Table 1). Yet it should be noted that 8C8 retains its ability to hydrolyze the (+) isomer, albeit at a significantly slower rate relative to (-)-CMP.

Since a 4th generation library, generated and screened similarly, did not reveal significant improvement over 8C8, we designed substitution-saturation libraries based on the observation that mutations at H115 and H134 (the His dyad) seem to display an allosteric effect that displaces the catalytic Ca^{2+} away from its coordinating residues (see milestone #3 below). Saturation mutagenesis at selected positions utilized the rePON1 gene bearing the H115W mutation, and active mutants were selected from this library using FACS (by means of the double-emulsion technique) and racemic CMP. Positive clones were grown in 96-well plates, followed by activity measurements using the (-)-CMP isomer. The following four key mutations were found to be associated with enhanced activity towards the (-) isomer: L69G/A, H115W, H134R, and F222S. These residues, that control stereo-selectivity towards OP substrates, appear to be on one side of the catalytic cavity of rePON1. These mutants were shuffled by random mutagenesis at a low rate, and sorted by FACS. Some of the most active variants were purified and analyzed. The results are summarized in Table 1.

Table 1 shows that in most of the improved variants, we found five key mutations, viz., L69G, H115W, H134R, F222S and T332S. However, the latter position is facing H115W on the opposite face of the cavity. One variant, 3D8, has an additional mutation, M196V, on the same side as the 4 mutations, L69G/A, H115W, H134R, and F222S. 3D8 is, thus far, the most active variant, exhibiting a k_{cat}/K_m value of >10^7 $M^{-1}min^{-1}$,viz., >4x10^5-fold greater than the wt G3C9 variant, which displays extremely low activity on (-)-CMP. The K_m value of 3D8 (25 μM) indicates high affinity for the enzyme, making it a most suitable candidate for in vivo detoxification. In addition, 3D8 is ~50 fold more selective for (-)-CMP than for its non-toxic enantiomer, (+)-CMP, a difference that might be utilized to isolate large quantities of the (+)-CMP isomer by the chemo-enzymic protocol described above for purification of (-)-CMP. Overall, the 3D8 variant had the broadest specificity for the *O*-cyclohexyl, *O*-isopropyl and *O*-ethyl toxic isomers of methylphosphonyl coumarin, i.e. the (-) enantiomers, with the following k_{cat}/K_m values: 11.6x10^6, 4.6x10^6, and 6.2x10^6 $M^{-1}min^{-1}$, respectively.

We thus demonstrated the potential of an enhanced evolution strategy, combining random and designed mutations, to yield a mutant with catalytic proficiency approaching the value that qualifies a catalytic bioscavenger as a candidate drug for pre-treatment of OP intoxication (k_{cat}/K_m ~ $5x10^7$ $M^{-1}min^{-1}$). The next step was to examine the suitability of the coumarin derivatives used to select active mutants (i.e., IMP and CMP; see structures in Table 2) as model OP substrates for identification and selection of clones relevant to the primary mission of this project, namely, to evolve a rePON1 capable of rapidly hydrolyzing the corresponding G-agents. To this end, we generated, in situ, in dilute aqueous solutions, the fluoridate analogs of IMP and CMP in which the P-O-coumarin moiety had been replaced by a P-F bond. The procedure implemented is fully controlled, safe and non-hazardous. Following complete release of the expected amount of the coumarin leaving group by NaF, in aqueous solution, the concentrations of the toxic (-)-IMP-F and (-)-CMP-F isomers were determined by titration of a known concentration of Torpedo californica AChE (TcAChE), and were verified by measuring the bimolecular rate constants for inhibition of AChE by the in-situ-generated sarin and cyclosarin, which were found to be consistent with published data. k_{cat}/K_m values were determined by monitoring the loss of anti-TcAChE potency of the freshly generated fluoridates, assuming that Km is well above the concentration of the tested (-)-IMP-F and (-)-CMP-F which were held at 30-50 nM. Table 2 shows that mutants 0C9, 2D8, and 1A4 are 3-4-fold more potent towards (-)-cyclosarin than the corresponding coumarin analog, and all three variants catalyzed its hydrolysis with values of k_{cat}/K_m >$1x10^7$ $M^{-1}min^{-1}$. They were found to be only 3-to 4-fold less potent in catalyzing the IMP-fluoridate (sarin) when compared to IMP-coumarin. Thus, the observed broad specificity and high proficiency confirmed our assumption that the OP-O-coumarin substrates serve as reasonable predictors in the screening of PON1 variants for the capacity to detoxify G-type nerve agents. In view of the inability of human PON1 to hydrolyze *O*-pinacolyl methylphosphonyl-O-coumarin (PinMP) (i.e., the soman analog model compound; Blum et al. [2008] *Biochemistry* 47:5216-5224), it will be important to test the mutants listed in Table 2 on both PinMP-O-coumarin and on soman itself. Results shown in Table 2 should be verified using aqueous solutions of neat nerve agents at USAMRICD, Aberdeen, MD. Our data call for development of a protocol for screening existing and future libraries with the in-situ-generated fluoridates, which will permit direct sorting of mutants capable of efficiently hydrolyzing G-agents.

Finally, neutral drift libraries (Gupta and Tawfik [2008] *Nat Methods* 11:939-42) selected with racemic CMP yielded a variant, 1G3, bearing the following mutations, T126A, A187V, F222S, H251N, Y293S, T332S. 1G3, like 3B3, catalyzed the hydrolysis of (+)-CMP with kcat/Km = 1.8x107 M-1min-1, viz., 70-fold faster than the wt G3C9. This mutant, which was mentioned in our year-2 report, was re-expressed, purified, its mutations confirmed, and following evaluation of its kinetic constants, delivered to USAMRICD (see below milestone #2).

03 Milestone #2. Transfer of a minimum of 3 promising candidates (in addition to 2B4 and 3B3) to USAMRICD for testing with G and V-type nerve agents

Plasmids of variants 8C8, 2H4, and 1G3 were delivered for further evaluation against 'live' nerve agents at USAMRICD.

In addition, the following rePON1 mutants were expressed and purified in our laboratory, and transferred to USAMRICD on early March 2009: 2C3, 3D8, 8C8, 1G3, 3B3, 2H4, 0C9, 2D8 and 1A4.

03 Milestone #3. Provide detailed 3D structures of the H115W mutant and of the H115Q/H134Q double mutant of recombinant PON1

H115W, which displays enhanced hydrolysis of compounds containing the P-S bond, such as found in the nerve agent VX, and the H115Q/H134Q double-mutant, that is almost devoid of lactonase and aryl esterase activity (both mutants originate from the G2E6 variant), were over-expressed and crystallized, followed by determination of their crystal structures by X-ray crystallography. Examination of their 3D structures revealed the following:

a. Movements of amino-acid side-chains and of the catalytic Ca+2 in the crystal structures of H115W and H115Q-H134Q relative to the wt PON1.

1. Movement of the catalytic Ca^{+2} by 1.7 Å (Fig. 4A)
2. No changes observed in the side-chains coordinating to the structural Ca^{+2} (Fig. 4B)
3. Whereas N224, N168 and N270 interact with the catalytic Ca^{+2} in the wt, they do not interact in either mutant (Fig. 5)
4. Changes are seen in both mutants in the orientations of residues N224 and E53

b. The Histidine dyad: H115, H134

1. Two alternative conformations (each at ~50% occupancy) were observed for H115 in the wt structure for which X-ray data were collected at pH 6.5, suggesting that the imidazole ring is mobile, and that there is ample free space to accommodation the corresponding conformers (Fig. 6A)

2. The movement of the side-chains of mutated residues at position 115 is approximately towards the position of the alternative conformation of H115 in the observed structure of the wt enzyme collected at pH 6.5 (Fig. 6B).

The 3D structures suggest that the mutations at H115 and H134 have an allosteric effect that results in displacement of the catalytic Ca^{2+} from its coordinating residues in the wt enzyme, viz., E53, D269, N168, N224 and N270. The movement of the catalytic Ca^{2+}, together with changes in the size and polarity of sub-sites in the active mutants identified (Table 1) may be correlated with both the enhancement of OPH activity and the reversal of stereo-selectivity. This suggests that construction of PON1 libraries based on the amino acid residues mentioned above, that coordinate to the catalytic Ca^{2+} ion in wt rePON, may produce improved PON1 mutants, and permit dissection of the structural features influencing binding and catalysis. Also, the presence of the phosphate ion, and its coordination to the catalytic Ca^{2+} in wt PON1, suggests that the catalytic Ca^{2+} may serve as an oxyanionic site for the tetrahedral OP substrate.

Additional progress in year 3:

(a) We have demonstrated by in vitro and in vivo studies (in collaboration with BioLine RX, Israel), both the improved thermal stability (ΔTm of 13^{o}C in favor of rePON1 over-expressed in E coli) and the antidotal efficacy of rePON1, compared to PON1 purified from human serum, when tested against intoxication of mice with chlorpyrifos-oxon.

(b) In order to provide an independent source for the (+) and (-) isomers, we developed a stereo-specific protocol for the synthesis of the two enantiomers of $CH_3P(O)(OC_2H_5)$-O-coumarin (EMP). The (+) and (-) isomers were crystallized, and their absolute configurations were established by X-ray crystallography (Fig. 7).

Key Research Accomplishments

- Mutants capable of hydrolyzing both isomers of CMP-coumarin and CMP-fluoride with values of k_{cat}/K_m >1x10^7 $M^{-1}min^{-1}$.
- Libraries of saturation-substitution mutants of rePON1, and a FACS screening protocol.
- 3D structures of wt rePON1 and of the two variants, H115W and H115Q/H134Q.
- Protocol for a controlled, safe and non-hazardous procedure for conversion of CMP and IMP bearing the coumarin leaving group to the corresponding fluoridates.
- Protocols for (a) stereo-specific synthesis of a chiral *O*-ethyl methylphosphonate with a 3-cyano-7-hydroxy-4-methylcoumarin leaving group (EMP); (b) Chemo-enzymic isolation of large quantities of a highly purified (-)-CMP derivative with a 3-cyano-7-hydroxy-4-methylcoumarin leaving group.

Reportable Outcomes

Manuscripts:

1. Devi-Gupta, R. & Tawfik, D.S. (2008) Directed enzyme evolution via small and effective neutral drift libraries. *Nature Methods* 11: 2311-2318. (attached)
2. Tokuriki, N. & Tawfik, D.S. (2008) GroEL/ES chaperonins promote genetic variation and accelerate enzyme evolution. *Nature* (under revision)
3. Ashani, Y., Ben-David, M., Devi-Gupta, R., Greenblatt, H.M., Leader, H., Mullokandov, G., Silman, I., Tawfik, D.S., and Sussman, J.L. (2008) Biochemical and Structural Analyses of Chiral Methylphosphonate Analogues of G- and V-agents for High-Throughput Screening of Reversed Stereoselectivity of Paraoxonase-1 Variants, Presentation at the 16th Biennial Medical Defense Bioscience Review, USAMRICD, June 1-6, Marriott Hotel, Hunt Valley MD
4. Colletier, J.-P. et al Sussman, J.L., Silman, I. & Weik, M. (2008). Shoot-and-Trap: Use of specific x-ray damage to study structural protein dynamics by temperature-controlled cryo-crystallography. *PNAS* 105, 11742-7. (attached)
5. Xu, Y. et al Silman, I. & Sussman, J.L. (2008). Flexibility of Aromatic Residues in the Active-Site Gorge of Acetylcholinesterase: X-ray versus Molecular Dynamics. *Biophys J* 95, 2500-11. (attached)
6. Xu, Y. et al Silman, I., Sussman, J.L. & Weik, M. (2008). Induced-fit or pre-existing equilibrium dynamics? Lessons from protein crystallography and MD simulations on acetylcholinesterase. *Protein Sci* 17, 601-5. (attached)

Conclusions

The model OP compounds and the in situ generation of G agents together with the screening approach that we developed and the libraries that were generated, established our methodologies for future screening and identification of promising PON variant candidates. Promising candidates were transferred to ICD to be tested with threat agents.

References

Aharoni, A., Gaidukov, L., Yagur, S., Toker, L., Silman, I., and Tawfik, D.S. 2004. Directed evolution of mammalian paraoxonases PON1 and PON3 for bacterial expression and catalytic specialization. *Proc. Natl. Acad. Sci. USA* 101: 482-487.

Amitai, G., Adani, R., Yacov, G., Yishay, S., Teitlboim, S., Tveria, L., Limanovich, O., Kushnir, M., and Meshulam, H. 2007a. Asymmetric fluorogenic organophosphates for the development of active organophosphate hydrolases with reversed stereoselectivity. *Toxicology* 233: 187-198.

Amitai, G., Devi Gupta, R., and Tawfik, D.S. 2007b. Latent evolutionary potentials under the neutral mutational drift of an enzyme. *HFSP Journal* 1: 67-78.

Yeung, D.T., Lenz, D.E., and Cerasoli, D.M. 2005. Analysis of active-site amino-acid residues of human serum paraoxonase using competitive substrates. *FEBS J.* 272: 2225-2230.

Tables

Table 1. Catalytic efficiency of mutants selected from substitution library variants by (-)-CMP. Values shown are k_{cat}/K_m ($\mu M^{-1}min^{-1}$)

Variant	(-)-CMP	(-)/(+) ratio for CMP	(-)-IMP	Mutations
8C8	0.093±0.003 (1)[a]	27	0.022(1)[a]	L69S, V97A, H115W, P135A, F222S
2C3	0.7±0.01 (7.5)	8	0.079(3.6)	L69G, H115W, H134R, F222S, K233E
5H5	1.25±0.05 (13.4)	6	0.76(35)	L10S, F28Y, L69G, H115W, H134R, F222S, T332S
0C9	2.85±0.1 (31)	9	1.04(47)	L14M, L69G, S111T, H115W, H134R, F222S, T332S
2D8	3.52±0.13 (38)	7.5	0.85(39)	L69G, H115W, H134R, F222S, T332S
1A4	3.63±0.1 (39)	9.5	0.85(39)	A6E, L69G, H115W, H134R, F222S, K233E, T332S, T326S
3D8	11.6±0.23 (125)	47	4.6(209)	L69G, H115W, H134R, M196V, F222S, T332S

a. Figures in parentheses show enhancement relative to the 8C8 variant

Table 2. Comparison of catalytic activity on an OP-coumarin model compound of rePON1 variants selected from a saturation library by use of (-)-OP-coumarin compounds (see Table 1), and their OP-fluoridate analogs. The figures shown are values of kcat/Km x106 M-1min-1 analogs

Mutant	(-)CMP-coumarin	(-)CMP-fluoridate	fluoridate/ coumarin	(-)IMP-coumarin	(-)IMP-fluoridate	fluoridate/ coumarin
8C8	0.09	0.2	2.2	0.02	0.03	1.5
3D8	11.6	3.3	0.3	0.46	0.10	0.2
0C9	2.8	11.1	3.9	1.04	0.32	0.3
2D8	3.5	14.3	4.1	0.85	0.23	0.3
1A4	3.6	11.3	3.1	0.85	0.21	0.25
2C3	0.7	0.47	1.5	0.08	0.02	0.25

1. Data for OP-coumarin are based on release of the chromophore monitored at 400 nm.
2. The k_{cat}/K_m values for the fluoridates were determined by monitoring the rate of loss of anti-AChE potency of the *in situ*-generated compound, assuming $K_m >> [P\text{-}F]$. Calculations are based on a single enzyme concentration selected to allow convenient and reliable determination of the apparent k_{obs} of loss of anti-AChE potency.
3. The coumarin leaving group is displaced by fluoride from the racemic coumarin-containing OPs to yield CMP-fluoride and IMP-fluoride. It should be noted that for both types of OP the above data relate to the toxic (-) isomers

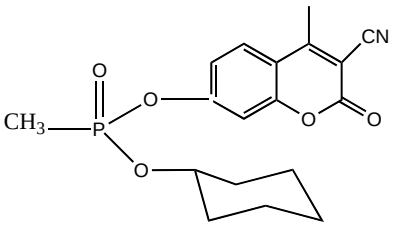

CMP-coumarin

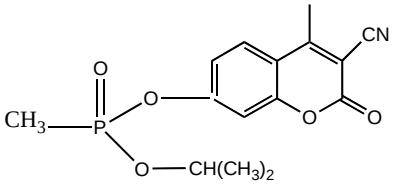

IMP-coumarin

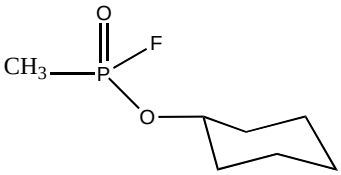

CMP-fluoride

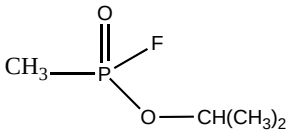

IMP-fluoride

Figures

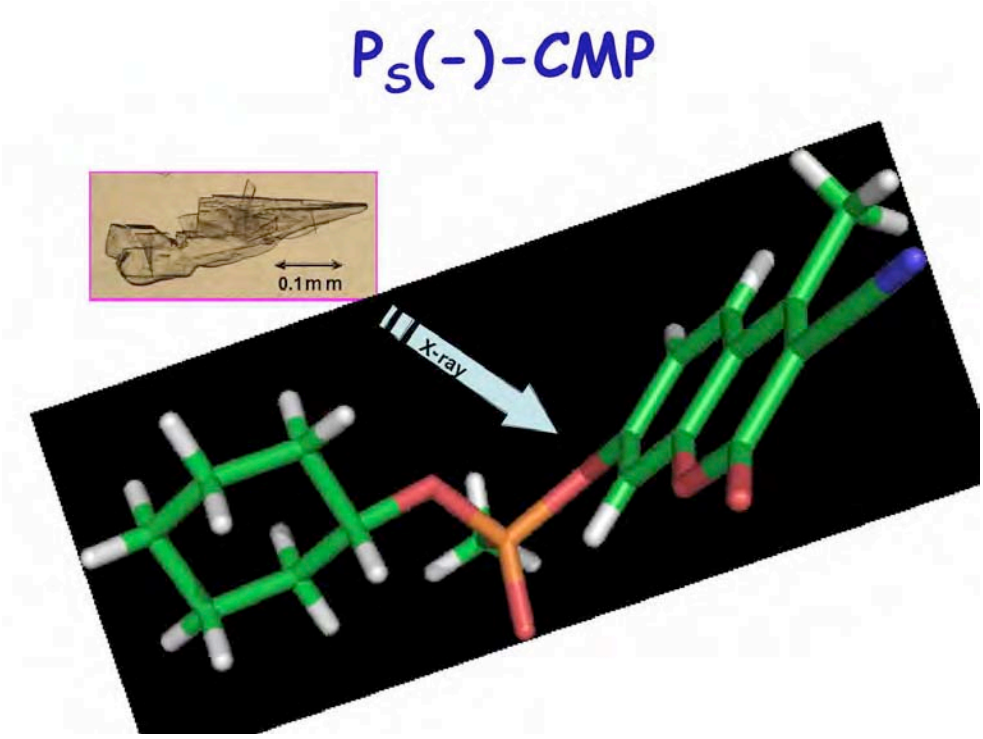

Figure 1. 3D structure of (-)-CMP

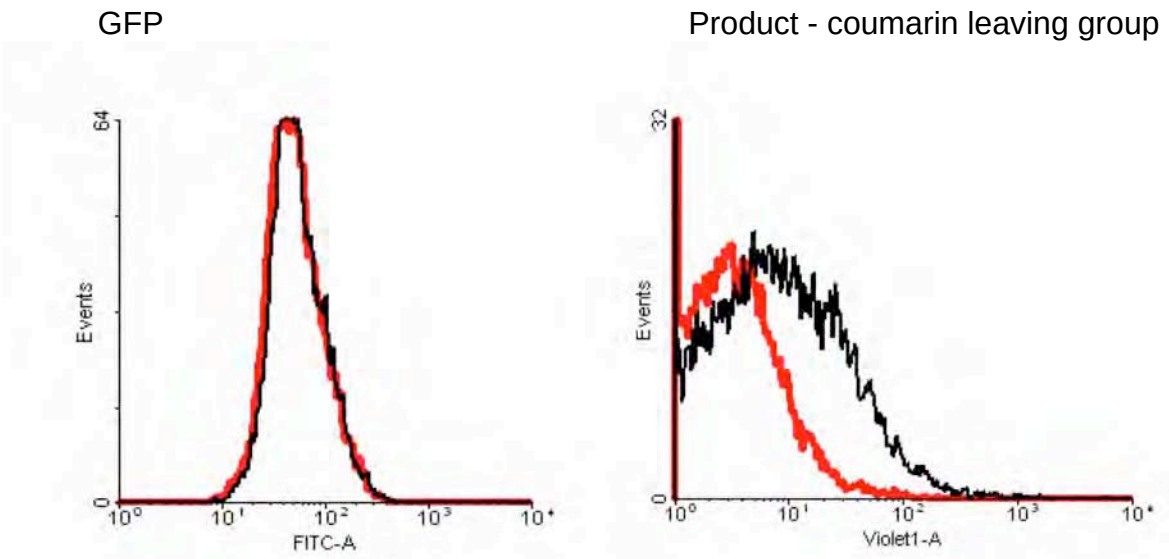

Figure 2. Sorting the double emulsion on FACS with (-)-CMP. Red - library; Black - positive controls

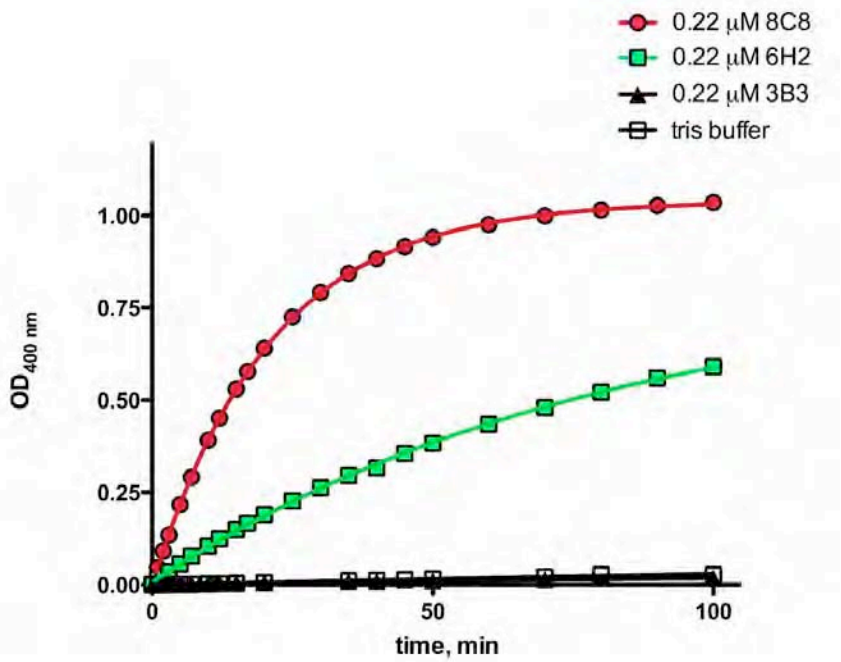

Figure 3. Reversed stereo-preference towards (-)-CMP displayed by mutants 8C8 and 6H2, as opposed to mutant 3B3, that essentially hydrolyzes only the (+)-CMP isomer

Pink, wt rePON1, pH 4.6; Grey, H115W, pH 6.5

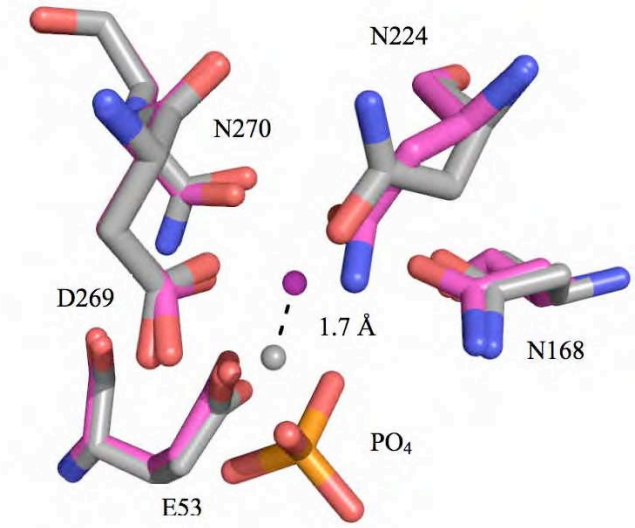

Figure 4a. Movement of the catalytic Ca+2 ion by 1.7 Å

Pink, wt, pH 4.6; green, wt, pH, 6.5; grey, H115W, pH 6.5; orange, H115Q/H134Q, pH 6.5

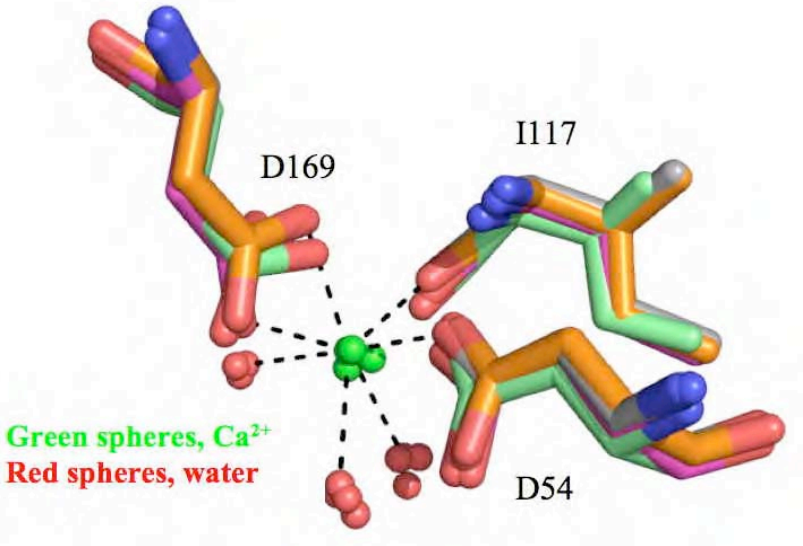

Figure 4b. Superposition of the structural Ca^{2+} ion of PON1 variants

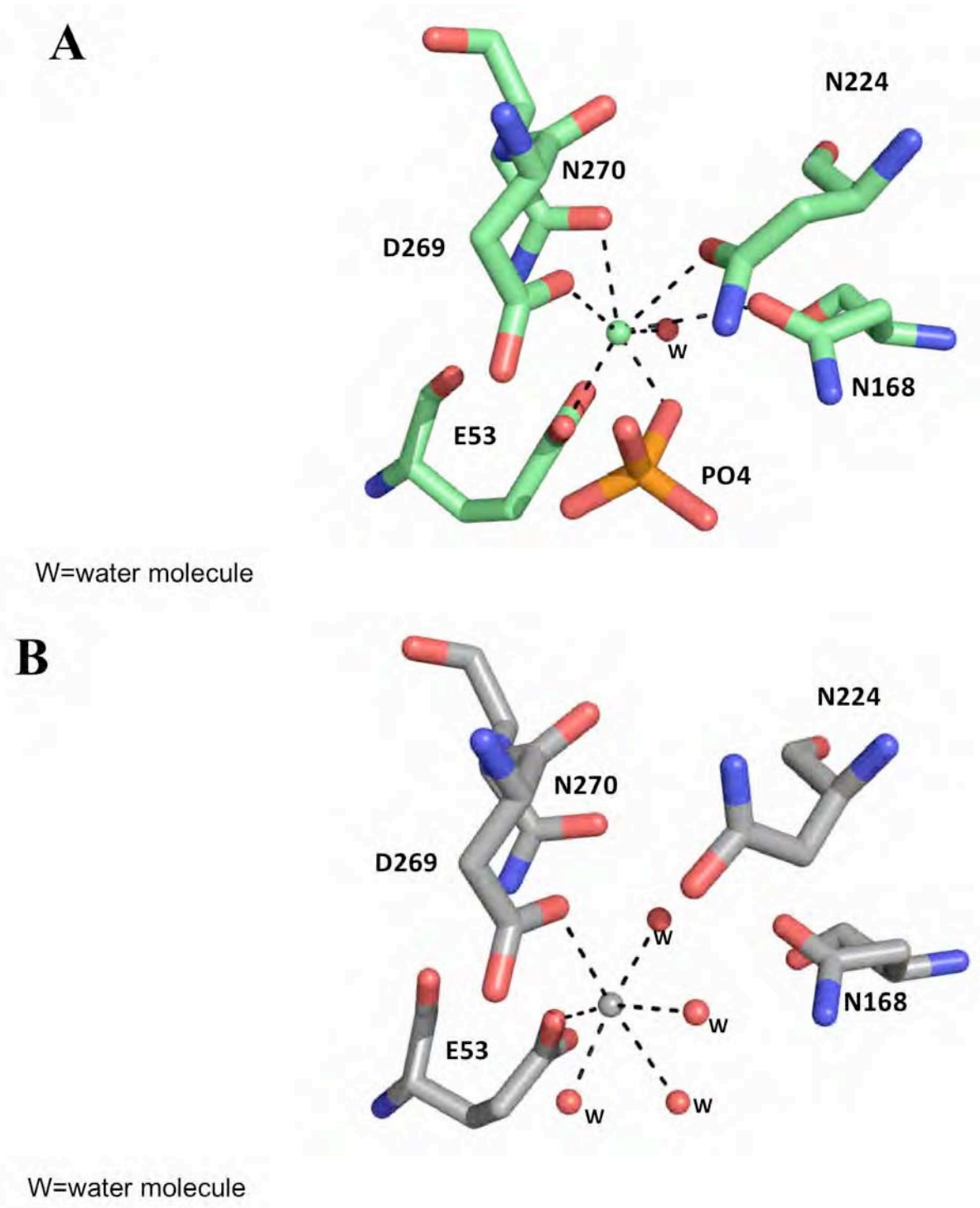

Figure 5. The catalytic Ca^{2+} site of wt rePON1 (A) and H115W (B) (both at pH 6.5), showing the changes in coordination to the Ca^{2+} ion.

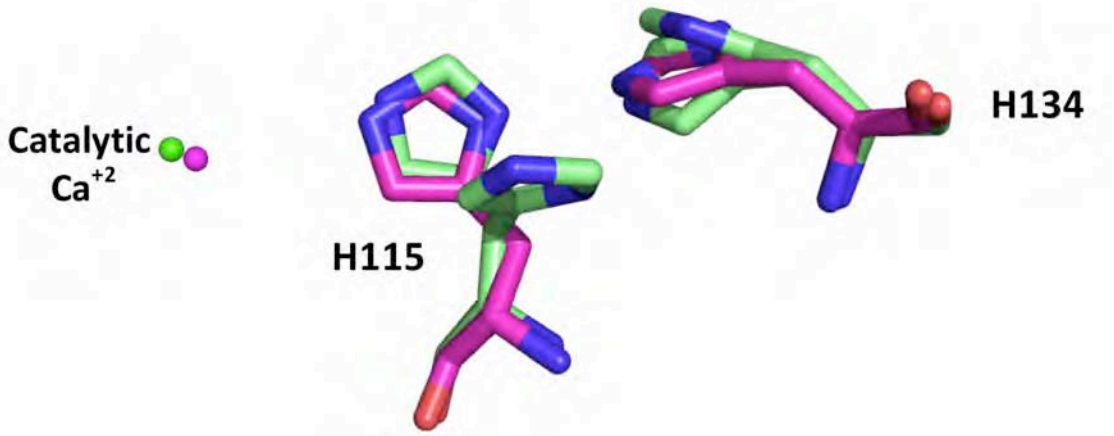

Figure 6a. Conformational mobility of the H115/H134 of wt rePON1 at pH 6.5 (green), compared to pH 4.6 (pink)

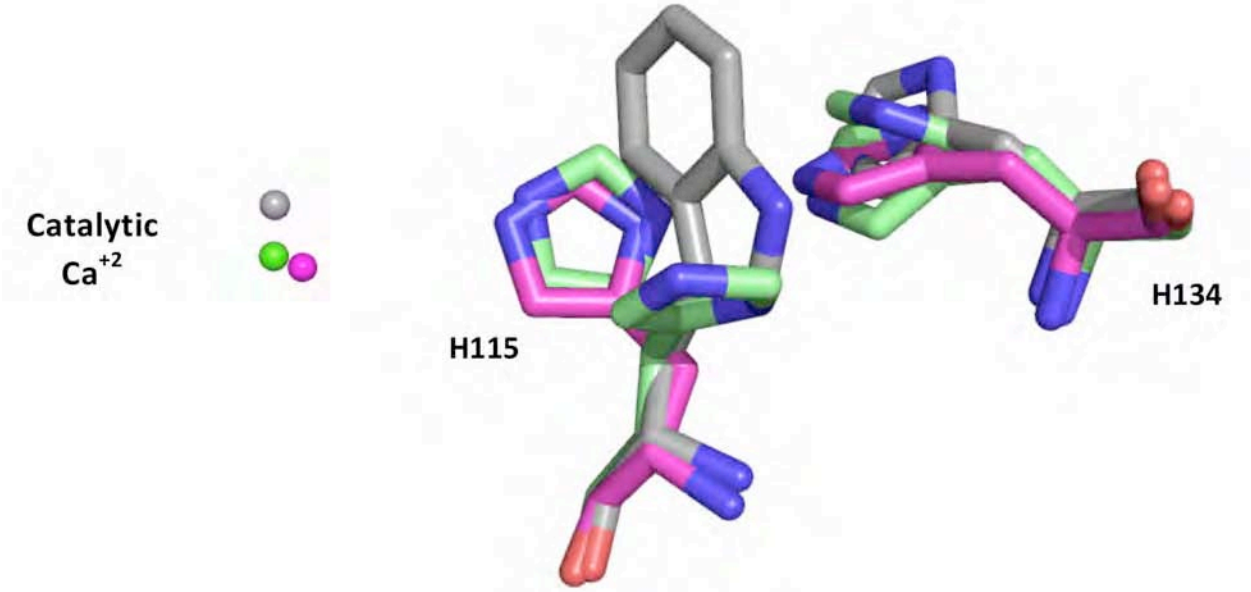

Figure 6b. Superposition of mutant H115W (grey) and wt rePON1 at pH 4.5 (pink) and pH 6.5 (green)

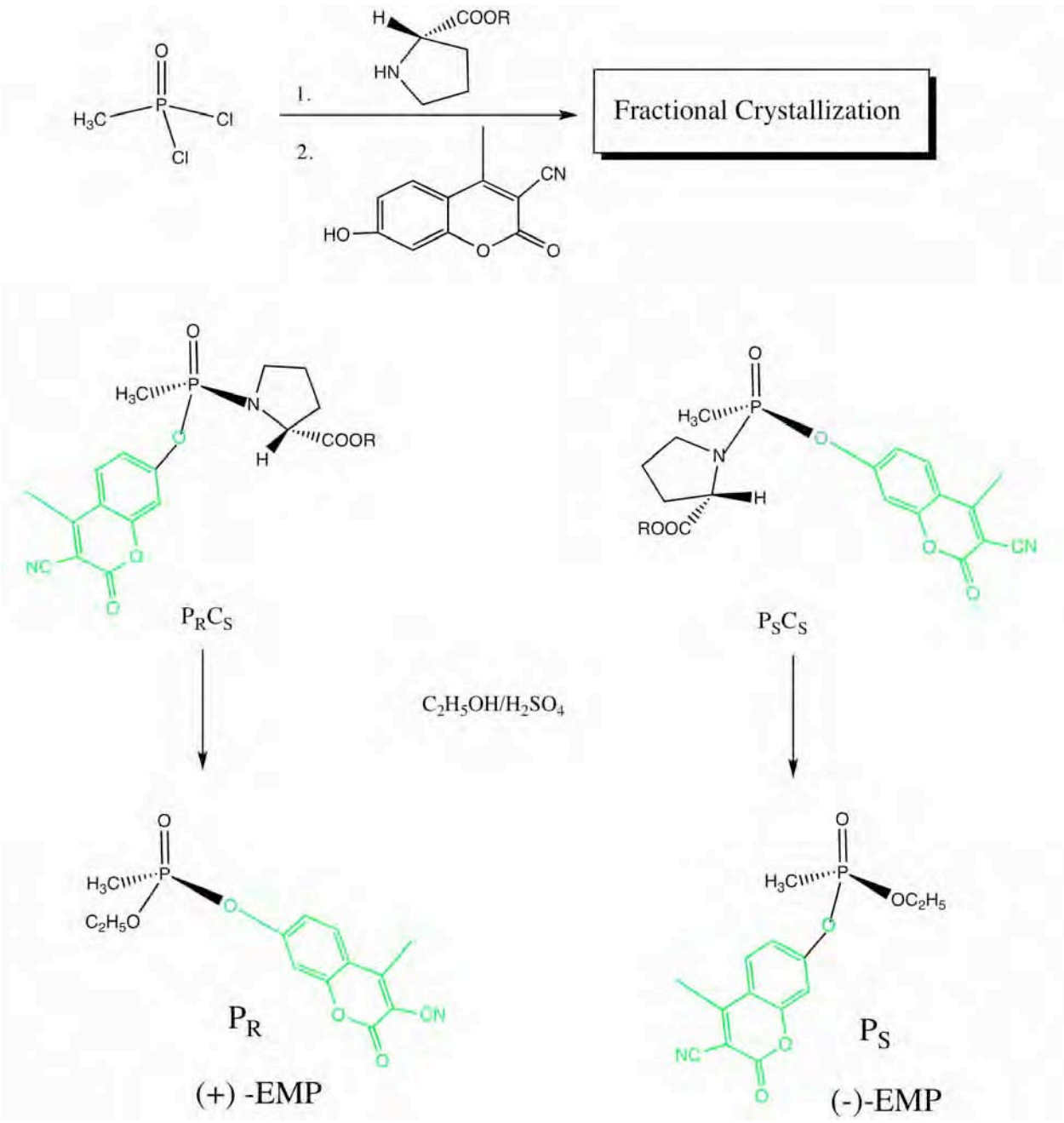

Figure 7. Stereo-specific synthesis of (+)- and (-)-EMP